[논 문] 한국재료학회지
Korean J. Mater. Res.
Vol. 26, No. 3 (2016)

http://dx.doi.org/10.3740/MRSK.2016.26.3.123

Synthesis and Characterization of TiO_2, Cu_2O and Al_2O_3 Aerosol Nanoparticles Produced by the Multi-Spark Discharge Generator

Alexey Efimov†, Anna Lizunova, Valentin Sukharev and Victor Ivanov

Department of Physical and Quantum Electronics, Moscow Institute of Physics and Technology, Dolgoprudny, Russia

(Received September 17, 2015 : Revised November 25, 2015 : Accepted January 21, 2016)

Abstract The morphology, crystal structure and size of aerosol nanoparticles generated by erosion of electrodes made of different materials (titanium, copper and aluminum) in a multi-spark discharge generator were investigated. The aerosol nanoparticle synthesis was carried out in air atmosphere at a capacitor stored energy of 6 J, a repetition rate of discharge of 0.5 Hz and a gas flow velocity of 5.4 m/s. The aerosol nanoparticles were generated in the form of oxides and had various morphologies: agglomerates of primary particles of TiO_2 and Al_2O_3 or aggregates of primary particles of Cu_2O. The average size of the primary nanoparticles ranged between 6.3 and 7.4 nm for the three substances studied. The average size of the agglomerates and aggregates varied in a wide interval from 24.6 nm for Cu_2O to 46.1 nm for Al_2O_3.

Key words nanoparticles, synthesis, aerosols, multi-spark discharge.

1. Introduction

Properties of nano-sized particles suspended in gaseous medium, or aerosol nanoparticles, are an important subject of research due to their wide application in various technologies of new materials and devices.[1] Properties of nanoparticles determine functional characteristics of many modern products and devices, such as electrodes for lithium-ion batteries[2] and supercapacitors,[3] luminophores,[4] drugs,[5] printed electronics products[6] and various functional coatings.[7] The rapid development of technological applications of aerosol nanoparticles stimulates targeted research of methods for their synthesis and characterization. Each of the known gas-phase methods of synthesis of nanoparticles, for example, the electrical explosion of conductors,[8] synthesis in a flame,[9] plasma,[10] laser,[11] spark discharge[12] and thermal evaporation[13] has inherent limitations for the kind of evaporated source material, size of the resulting nanoparticles and energy efficiency.

Recently, due to the need for expanding opportunities for the production of nanoparticles and obtaining a stable flow of aerosols,[14] a method of nanoparticle synthesis in pulsed spark discharge, where the nanoparticles are generated by electrical erosion of the electrode material, has been developed.[15,16] The distinctive features of this method are: a) the possibility of the synthesis of very small primary nanoparticles with a diameter of less than 10 nm from metals,[12,17] oxides,[18] semiconductors[19] and carbon materials[20]; b) high chemical purity of the synthesized nanoparticles with a low content of impurities[15]; c) the relative simplicity of the implementation of the method.[12] Moreover, the synthesis of nanoparticles in a spark discharge allows to control the size of the particles by changing the energy stored in the capacitor, repetition frequency of discharges and gas flow rate.[15] Until recently, the synthesis of nanoparticles by this method was limited to the use of spark discharge in the mode of self-breakdown of electrode gap.[12] Such mode was unstable for generation of particles with the required size distribution, energetically inefficient and low-productive.[12,21,22] In the development of this method a controlled breakdown of the multiple electrode gaps, connected in series in a single discharge circuit, was implemented to ensure the stability of the dimensional parameters of the obtained nanoparticles.[23] Previously, physics of a pulsed breakdown of gas and vacuum gaps was developed in order to create large pulsed power generators, electron accelerators and microwave generators.[24] The present study of the syn-

†Corresponding author
E-Mail : efimov.aa@mipt.ru (A. Efimov, Moscow Institute of Phys & Technol.)

thesis of nanoparticles in a spark discharge is based on the similar physics. In particular we demonstrate implementation of a controlled cascade breakdown of discharge gaps utilizing the effect of electric field distortion by applying a trigger discharge pulse to the central control electrode.[24] Such switching circuit is characterized by a wide range of operating voltages for a fixed gap between the electrodes in contrast to the self-breakdown mode and it improves the time stability of the mass production of nanoparticles and their particle size distribution.[23]

Despite advances in the understanding of the basic mechanisms of the formation of nanoparticles in gases,[25,26] prediction of particle size, the rate of formation and the degree of aggregation based on the first principles is difficult and not always a feasible task for the synthesis in a spark discharge. Therefore comprehensive experimental investigation of dimensional and structural characteristics of the nanoparticles generated by the erosion of the electrodes of different materials is required.

The aim of this study is to find the relationship between the properties of aerosol nanoparticles synthesized by electrical erosion of the electrodes in a spark discharge and properties of the electrode materials. This paper investigates the morphology, the crystal structure, the size of the primary particles and agglomerates/aggregates of aerosol nanoparticles generated by erosion of different metal electrodes: Ti, Cu and Al. These materials were chosen because of the wide range of applications and useful properties of their nanosized oxides: TiO_2 nanoparticles have unusual chemical and photocatalytic properties,[27] semiconducting Cu_2O nanoparticles are a promising material for solar energy,[28] widely used in electronics[29] and catalysis[30]; Al_2O_3 nanoparticles have special properties such as heat resistance and high hardness of these nanoparticles are widely used for the production of various ceramic materials.[31] Investigation of the relationship between the properties of nanoparticles obtained in a spark discharge and the electrode material is an important fundamental issue for understanding and predicting the properties of nanoparticles and their potential applications. It is known that the crystal structure of the TiO_2 nanoparticles depends on their size,[32] and the particles of the anatase phase have higher photocatalytic activity than, for example, particles of the rutile phase.[33] Average particle size and morphology of the nanoparticles synthesized according to the electrode materials is also an urgent task. For example, single monodisperse nanoparticles are used primarily in sensors[34] and optoelectronic devices,[35] while for the production of nanocomposites, reinforcing additives and paints nanoparticles in the form of agglomerates are preferred,[36] and aggregates of particles are better suited for the creation of a number of catalysts.[37]

The novelty of the current study is the synthesis of nanoparticles of oxides of aluminum, titanium and copper using a multi-spark discharge generator with a controlled trigger discharge mode. In addition, we demonstrate the difference of properties of the nanoparticles obtained in the multi-spark discharge generator compared to a conventional spark generator operating in self-breakdown mode.

2. Experimental Procedure

Schematic diagram of multi-spark discharge generator for production nanoparticles is presented in Fig. 1.

The source electrodes were metal cylinders with a nominal diameter of 10 mm made of Ti, Cu and Al (Fig. 1). Pulse energy release in the discharge gaps in the near-electrode zones led to the erosion of the electrode material with the subsequent formation of nanoparticles. The electrode gaps were purged by a purified stream of dry air (Fig. 1). Sampling of the aerosol for measurements of the nanoparticles was carried out using tubes connected to the aerosol spectrometer and the electrostatic sampler for collection nanoparticles (Fig. 1). Characterization of the collected nanoparticles was performed using transmission electron microscope (TEM) JEM-2100 (JEOL Ltd.), lattice parameters and structure of the particles was studied by the selected area electron diffraction (SAED) and nanodiffraction (NBD).

For the experiments we used a multi-spark discharge

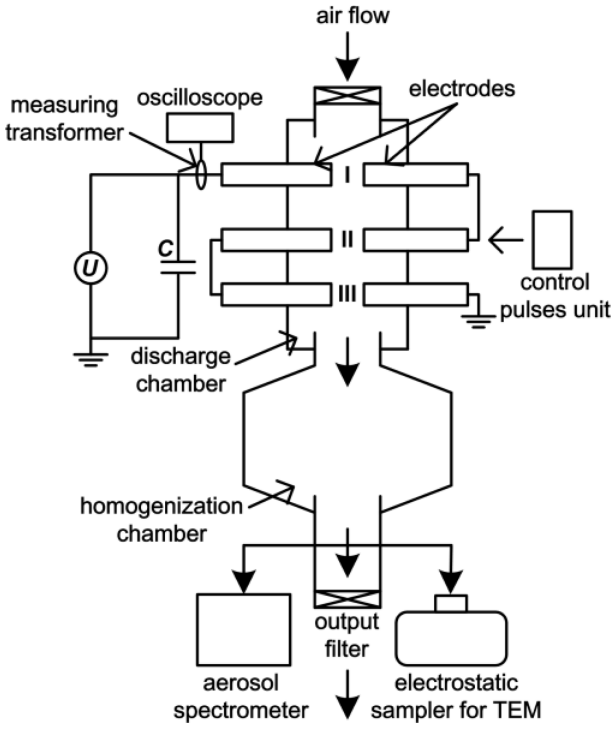

Fig. 1. A schematic diagram of the multi-spark discharge generator for producing aerosol nanoparticles.

Table 1. The result of optimization of the mode of synthesis of nanoparticles by the multi-spark discharge generator at the capacitance of the capacitor (C) and the distance between the titanium electrodes (l_{gap}) of 1.0 μF and 0.5 mm, respectively.

Air flow velocity v (m/s)	Energy stored on a capacitor W (J)	Repetition rate of discharges f (Hz)	Average size by SMPS (nm)	Total number concentration 10^6 (cm^{-3})
1.4			56	3.9
3.4	2		37	3.1
		0.5	32	2.8
5.4	6		34	4.1
	18		48	9.1

Table 2. The parameters of the multi-spark and conventional discharge generators.[12,23,38,39]

Parameter	Multi-spark discharge generator	Conventional spark discharge generator
Trigger mode of discharge	by applying a trigger pulse[24]	without a trigger pulse
Operating voltage range	from 1/3 to 2/3 of the self-breakdown voltage	only self-breakdown voltage
Number of discharge gaps	3	1
Electrode spacing l_{gap} (mm)	0.5-6	0.5-2.5
Discharge voltage U (kV)	0.5-10	0.5-12
Capacitance C (nF)	100-1000	2-126
Energy stored on a capacitor W (mJ)	13-50,000	3-9,000
Repetition rate of discharges f (Hz)	0.5-10	10-300
Gas flow rate Q (l/min)	0-160	0-20

generator of aerosol nanoparticles[23] in the mode with fixed operating parameters: at capacitor stored energy of 6 J, a repetition rate of discharges of 0.5 Hz and an air flow velocity of 5.4 m/s (or 160 l/min). This mode of synthesis was optimized to obtain weakly agglomerated aerosol nanoparticles at high number concentration. The optimization results are presented in Table 1. Measurements of size and total number concentration of the nanoparticles in the aerosol flow was performed with the aerosol spectrometer SMPS 3936 (TSI Inc.). The uncertainty of measurements of size and concentration of aerosol nanoparticles did not exceed 11 % and 17 %, respectively.

Table 1 shows that the aerosol nanoparticles have a minimum size and total number concentration of 32 nm and $2.8 \cdot 10^6$ cm^{-3}, respectively, at the maximum air flow velocity $v = 5.4$ m/s, the minimum energy stored in a capacitor $W = 2$ J and the repetition rate of discharges $f = 0.5$ Hz. However, for further experiments the mode with $W = 6$ J, $v = 5.4$ m/s and $f = 0.5$ Hz was selected, because in these conditions the aerosol nanoparticles are synthesized at a high number concentration without significant changes in particle size.

It should be noted that distinctive features of this multi-spark discharge generator from the generators of other authors[12,18] is the presence of three series-connected spark gaps (I, II and III) and implementation of the controlled discharge via the control pulses unit (Fig. 1). It allows the breakdown of gas gaps at fixed charge voltage of capacitors and repetition rate of discharges without Tesla transformer.[20] The comparison of the main parameters of the multi-spark and conventional discharge generators are presented in Table 2.

Table 2 shows that the main feature of the multi-spark discharge generator is the use of a trigger pulse to control the discharge. This feature allows to obtain the electrical breakdown of the gap in a wider voltage range from 1/3 to 2/3 of the self-breakdown voltage.[40] Therefore it allows to operate at a constant production rate of aerosol nanoparticles with stable particle size distribution, because the breakdown voltage is less dependent on the distance between electrodes than in the case of self-breakdown mode.[23] Another distinctive feature of the multi-spark discharge generator is the use of high air flow rate (0-160 l/min) and low repetition rate of discharge (0.5-10 Hz), which leads to generation of smaller nanoparticles.[12] Theoretically, based on the established dependencies the introduction of three pairs of discharge gaps and using the higher values of energy stored in a capacitor, up to 50,000 J, can increase the mass productivity of nanoparticles by 3-20 times compared to conventional generator.[16,38]

3. Result and Discussion

Fig. 2 shows the aerosol nanoparticles synthesized from different electrode materials Ti, Cu and Al. They are either agglomerates of primary spherical particles as in the case of Ti and Al (Fig. 2a and c, respectively), or

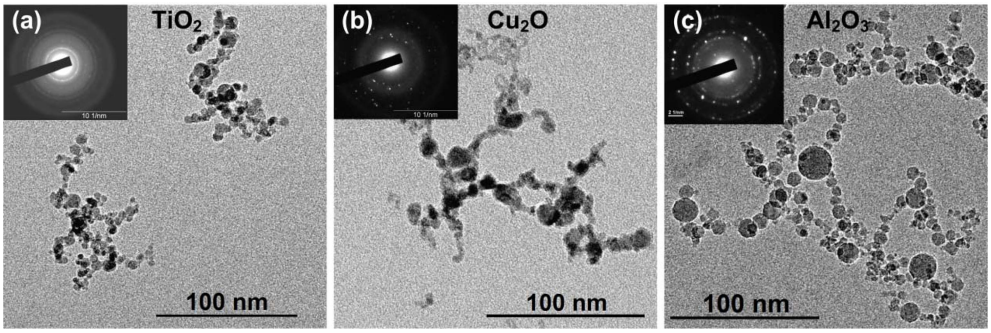

Fig. 2. TEM images of oxide nanoparticles and the corresponding electron diffraction pattern SAED (insertion) for (a) TiO_2, (b) Cu_2O and (c) Al_2O_3.

Table 3. Morphology, crystal structure and the average size of the nanoparticles synthesized by the multi-spark discharge generator.

Electrode (melting temperature)[43] (K)	Crystal structure of oxides	Types of nanoparticles morphology	Average primary particle size by TEM (nm)	Average agglomerates or aggregates size by TEM/SMPS (nm)
Ti (1941)	TiO_2 (anatase), tetragonal	agglomerates	7.4	26.8/31.0
Cu (1358)	Cu_2O, cubic	aggregates	7.6	20.6/24.6
Al (934)	Al_2O_3 (γ), cubic	agglomerates	6.3	44.9/46.1

aggregates of primary crystallites particles as in the case of Cu (Fig. 2b). The term primary particles here denote the smallest particles that can be discretely identified using a TEM. The term agglomerate means the combination of particles with weak interparticle interactions due to van der Waals forces or electrostatic forces, and the term aggregate means an assembly of particles with strong interparticle interactions through covalent, ionic or metallic bonds as defined in ISO 14887:2000.[41]

The average sizes of primary particles and agglomerates or aggregates, calculated from TEM-image analysis under the assumption of spherical objects, are presented in Table 3. The inaccuracies of determination of average size of nanoparticles from TEM and SMPS data do not exceed 4 and 7 %, respectively. Numerical size distribution of primary particles and agglomerates/aggregates are well approximated by functions of log-normal distribution, which is typical for gas-phase methods of nanoparticle synthesis.[42]

The results of image analysis of electron diffraction from agglomerates/aggregates and nanodiffraction from primary particles indicates the presence of the following crystalline modifications of nanoparticles obtained by erosion of the Ti, Cu and Al electrodes: TiO_2 anatase of the tetragonal system, Cu_2O and γ-Al_2O_3 with cubic lattices (Table 3). The generation of oxide nanoparticles from the respective electrode metals is justified as it occurs in oxygen-containing atmosphere.

The average size of primary particles was determined by analysis of about a thousand of primary particles to ensure the representativeness of the sample. The uncertainty of the measurement results of the average size of the primary nanoparticles did not exceed 4 %. The average sizes of primary particles according to the results of TEM-image analysis were: 7.4, 7.6 and 6.3 nm for Ti, Cu and Al electrodes, respectively (Table 3). Close values of sizes of primary particles obtained by pulsed electric erosion of the metal electrodes with significantly different physical and chemical properties, can be explained by the similarity of the physical nature of the pulsed electric discharge and/or fast relaxation process of electric-discharge plasma. The relative independence between the size of the primary nanoparticles and key physico-chemical parameters of the material was observed previously in the synthesis of nanoparticles by laser ablation. In the study of Ullmann et al[44] the average size of the primary nanoparticles produced by laser ablation was in the narrow range from 4.9 to 13 nm, despite significant differences in the properties of the target materials. Similar to the method of spark discharge there was no significant correlation between the size of primary nanoparticles and, for example, the melting temperature, or some other single physico-chemical parameter of the target material.[44] The constancy of the size of primary particles for different target materials most likely is due to a high cooling rate of the vapor within the collision-coalescence theory and is discussed in detail in the study of Friedlander,[45] Lehtinen and Zachariah[46] and Ullmann et al.[44]

The opposite trend is observed at a slow quasi-stationary evaporation and condensation of vapors of

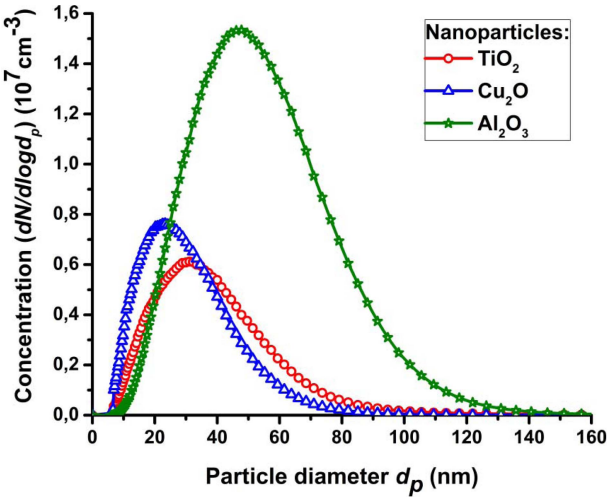

Fig. 3. Particle size distributions measured by SMPS for the aerosol nanoparticles TiO_2, Cu_2O and Al_2O_3 generated by the multi-spark discharge generator.

materials, for example, in the method of nanoparticle synthesis in a stationary flame,[9] where there is greater variability in the sizes of primary particles depending on the properties of evaporated material associated with the solid-state diffusion coefficients, melting and evaporation temperatures of materials. Particularly, in the synthesis of nanoparticles in flame[25,26] the size of primary TiO_2 and Al_2O_3 nanoparticles under identical synthesis conditions differed more than 2 times. In our work the difference in sizes of primary particles of such oxides does not exceed 1.2 times. A slight variation between the sizes of primary particles depending on the properties of evaporated target material is typical to the method of pulsed laser ablation,[44,47] as well. For example, in[44] the relation between the size of TiO_2 and Al_2O_3 primary particles synthesized by laser ablation in the same conditions was about 1.1. It is worth noting that the trend of increasing sizes of the primary particles from Al_2O_3 to TiO_2 is observed for both pulse methods.

Despite the small variation in the size of primary nanoparticles due to the type of electrode material, the size difference of the nanoparticle agglomerates and aggregates was more significant. In particular, the number average sizes of the agglomerates/aggregates of aerosol nanoparticles according to TEM were: 26.8, 20.6 and 44.9 nm for TiO_2, Cu_2O and Al_2O_3, respectively (Table 3). This data agrees well with the results of particle size measurement according to their electrical mobility by the aerosol spectrometer within an uncertainty of measurements (Table 3). Fig. 3 and data in Table 3 shows significantly different values of average sizes (from 24.6 to 46.1 nm by SMPS) and particle size distributions for aerosol nanoparticles generated from different electrode materials in the same mode.

It should also be noted that the electrode materials with a relative high melting point such as Ti and Cu result mostly in agglomerates/aggregates of particles with a small size of about 24.6 and 31.0 nm, respectively and materials with a relative low melting point such as Al result in strongly agglomerated particles with size up to 46.1 nm. This dependence is likely to be associated with a higher agglomeration of the nanoparticles due to their higher concentrations as a result of erosion of the electrode material with low melting point (Table 3). The correlation of size of the particle agglomerates/aggregates to the melting temperature of the electrode materials is significant. However, the physical base for aerosol nanoparticle synthesis in pulsed spark discharge is clearly more difficult. Apparently the formation of particles in the spark discharge also depends on such parameters as electrode materials enthalpy of evaporation[12] and oxidation, thermal conductivity,[48,49] and the ionization potential of a metal,[17] work function for electron emission[50] and optical properties[50] that determine the formation and absorption of radiation of the discharge. For example, one study[49] reported that for electrode materials with a high thermal conductivity coefficient electrodes evaporation was less intense due to the efficient cooling. The study[17] reported that from electrode materials with a high ionization potential of a metal, such as Au and Pt, nanoparticles were synthesized with a large primary particle size and a higher mass productivity. It is also known that materials with high enthalpy of evaporation and melting point,[12,51] such as W, are the most spark-resistant materials and demonstrate the lowest mass loss by electrical erosion. In our study, Ti and Cu were more spark-resistant compared to Al. Consequently, as a result of electrical erosion of Ti and Cu electrodes less aerosol nanoparticles with a smaller size of agglomerates/aggregates of particles were synthesized in comparison Al electrodes (Fig. 3 and Table 3). For the electrode materials with relatively high enthalpy of oxidation/formation of −944 (Al_2O_3) and −1676 kJ/mol (TiO_2),[43] the nanoparticles are obtained in the form of agglomerates and for Cu electrodes with low enthalpy of oxidation/formation (167 kJ/mol for Cu_2O),[43] nanoparticles are obtained in the form of aggregates (TEM-image in Fig. 2). This is due to the fact that the morphology of nanoparticles can influence the oxidation process of the particles. As a result of oxidation, the primary particles can be formed with an oxide shell or completely oxidized, which will protect against the formation of aggregates with strong chemical bonds between the primary particles.[52] However, it should be noted that the mechanism of nanoparticles formation in a spark discharge is complex and still not fully understood.

Since our generator has several distinctive features (see

Table 4. Properties of the nanoparticles synthesized in the multi-spark and a conventional discharge generator.

Reference	This study	Oh et al[53]	Byeon et al[54]	This study	Bau et al[39]	Jing et al[55]	This study	Bau et al[39]	Ghaemi et al[56]
Electrode material	Ti			Cu			Al		
Oxidation state	TiO_2			Cu_2O		CuO/Cu_2O	Al_2O_3		
Primary particle size (nm)	7.4	< 10	n/d	7.6	9	5	6.3	16	10
Agglomerate/aggregate size (nm)	31.0	49	43.3	24.6	6-18	17.6	46.1	8-50	n/d
Total number concentrate-on 10^6 (cm^{-3})	3.6	-	14.9	4.7	1-30	22.7	7.9	1-30	> 1
Morphology type	agglomerates	aggregates	n/d	aggregates			agglomerates	aggregates	
W, mJ	6000	5	5.8	6000	n/d	13	6000	n/d	n/d
f, Hz	0.5	50	1020	0.5	30-300	50	0.5	30-300	300
Q, (l/min)	160	0.3	3.2	160	0-20	4.75	160	0-20	4-6

Section 2), we performed a comparison of the properties of the nanoparticles from the multi-spark discharge and a conventional aerosol generator. The comparison results are presented in Table 4.

Table 4 shows that the multi-spark discharge generator produces comparable (in the case of CuO/Cu_2O) or usually smaller (in the case of TiO_2 and Al_2O_3) primary particles in comparison with the conventional spark discharge generator. For example, using the multi-spark discharge generator the size of synthesized primary particles of Al_2O_3 was 6.3 nm, while in the conventional spark discharge generator this size exceeded 10 and 16 nm depending on the specific study[39,56] (see Table 4). The Al_2O_3 nanoparticles were synthesized as aggregates in a conventional generator. In this study we obtained weakly agglomerated TiO_2 nanoparticles with sizes 40-60 % less than in other studies.[53,54] The synthesis of smaller nanoparticles may be caused by higher gas flow rate and lower repetition rate of discharges (160 l/min and 0.5 Hz, respectively). This leads to a more efficient dilution of aerosol particles, which was indirectly indicated by the results of measurements of the total number concentration, which were 4-6 times lower than in other studies.

4. Conclusion

We have studied characteristics (morphology, crystal structure and size) of aerosol nanoparticles of oxides of Ti, Cu and Al obtained by electrical erosion of metal electrodes in a controlled multi-spark discharge generator with constant parameters of the synthesis. Due to the controlled discharge and a serial connection of three pairs of discharge gaps in a single discharge circuit it was possible to achieve the stability of the dimensional parameters of the nanoparticles.

This work showed the prospects of development of the technology of multi-spark discharge generator for stable synthesis of primary nanoparticles with size of up to 10 nm required for a wide range of applications.

It is found that the size of the primary nanoparticles weakly depends on the materials of electrodes and is in the range from 6.3 to 7.6 nm for three materials studied. Similar sizes of primary particles synthesized by pulse electrical erosion of metal electrodes with significantly different physico-chemical properties can be explained by the commonality of the physical nature of the pulsed electric discharge and/or fast relaxation process of electric-discharge plasma. This result indicates the need for further research aimed at establishing the fundamental laws of particle formation in a pulsed spark discharge.

The size of the particle agglomerates/aggregates strongly depends on the electrode material and is in a wider range from 24.6 nm for Cu_2O to 46.1 nm for Al_2O_3. The aerosol nanoparticles obtained by erosion of the electrodes made of materials with relative higher melting points (Ti and Cu) are characterized by a smaller size of the agglomerates/aggregates.

Acknowledgment

This work was supported by a grant from the Russian Science Foundation (project No 15-19-00190).

References

1. F. E. Kruis, H. Fissan and A. Peled, J. Aerosol Sci., **29**, 511 (1998).
2. D. Liu and G. Cao, Energy Environ. Sci., **3**, 1218 (2010).
3. G. Wang, L. Zhang and J. Zhang, Chem. Soc. Rev., **41**, 797 (2012).
4. F. Wang, W. B. Tan, Y. Zhang, X. Fan, M. Wang, Nano-

technology, **17**, R1 (2006).
5. S. K. Murthy, Int. J. Nanomedicine, **2**, 129 (2007).
6. A. Kamyshny and S. Magdassi, Small, **10**, 3515 (2014).
7. C. Boissiere, D. Grosso, A. Chaumonnot, L. Nicole and C. Sanchez, Adv. Mater., **23**, 599 (2011).
8. Y. A. Kotov, Nanotechnol. Russ., **4**, 415 (2009).
9. L. Mädler, H. K. Kammler, R. Mueller and S. E. Pratsinis, J. Aerosol Sci., **33**, 369 (2002).
10. D. Vollath, J. Nanopart. Res., **10**, 39 (2008).
11. V. V. Osipov, Y. A. Kotov, M. G. Ivanov, O. M. Samatov, V. V. Lisenkov, V. V. Platonov, A. M. Murzakaev, A. I. Medvedev and E. I. Azarkevich, Laser Phys., **16**, 116 (2006).
12. N. S. Tabrizi, M. Ullmann, V. A. Vons, U. Lafont and A. Schmidt-Ott, J. Nanoparticle Res., **11**, 315 (2009).
13. B. K. Ku and A. D. Maynard, J. Aerosol Sci., **37**, 452 (2006).
14. http://www.buonapart-e.eu/
15. T. V. Pfeiffer, J. Feng and A. Schmidt-Ott, Adv. Powder Technol., **25**, 56 (2014).
16. B. O. Meuller, M. E. Messing, D. L. J. Engberg, A. M. Jansson, L. I. M. Johansson, S. M. Norlén, N. Tureson and K. Deppert, Aerosol Sci. Technol., **46**, 1256 (2012).
17. J. H. Byeon, J. H. Park, J. Hwang, J. Aerosol Sci., **39**, 888 (2008).
18. J. T. Kim and J. S. Chang, J. Electrostat., **63**, 911 (2005).
19. V. A. Vons, L. C. P. M. de Smet, D. Munao, A. Evirgen, E. M. Kelder and A. Schmidt-Ott, J. Nanopart. Res., **13**, 4867 (2011).
20. H. Horvath and M. Gangl, J. Aerosol Sci., **34**, 1581 (2003).
21. D. Z. Pai, K. Ostrikov, S. Kumar, D. A. Lacoste, I. Levchenko and C. O. Laux, Sci. Reports, **3**, 1221 (2013).
22. E. Hontañón, J. M. Palomares, M. Stein, X. Guo, R. Engeln, H. Nirschl and F. E. Kruis, J. Nanopart. Res., **15**, 1957 (2013).
23. A. A. Efimov, V. V. Ivanov, A. V. Bagazeev, I. V. Beketov, I. A. Volkov and S. V. Shcherbinin, Tech. Phys. Lett., **39**, 1053 (2013).
24. G. A. Mesyats, Pulsed power, Springer Science & Business Media, New York, USA(2007).
25. R. S. Windeler, S. K. Friedlander and K. E. J. Lehtinen, Aerosol Sci. Technol., **27**, 174 (1997).
26. R. S Windeler, K. E. J. Lehtinen and S. K. Friedlander, Aerosol Sci. Technol., **27**, 191 (1997).
27. D. A. H. Hanaor and C. C. Sorrell, J. Mater. Sci., **46**, 855 (2011).
28. A. O. Musa, T. Akomolafe and M. J. Carter, Sol. Energy Mater. Sol. Cells, **51**, 305 (1998).
29. P. Poizot, S. Laruelle, S. Grugeon, L. Dupont and J. M. Tarascon, Nature, **407**, 496 (2000).
30. H. Zhang, X. Ren and Z. Cui, J. Cryst. Growth, **304**, 206 (2007).
31. V. V. Ivanov, S. N. Paranin and V. R. Khrustov, Phys. Met. Met., **94**, S98 (2002).
32. V. G. Zhigalina, A. A. Lizunova, S. N. Sulyanov, V. V. Ivanov and N. A. Kiselev, Nanotechnol. Russ., **9**, 492 (2014).
33. T. Luttrell, S. Halpegamage, J. Tao, A. Kramer, E. Sutter and M. Batzill, Sci. Reports, **4**, 4043 (2014).
34. P. R. Solanki, A. Kaushik, V. V. Agrawal and B. D. Malhotra, NPG Asia Mater., **3**, 17 (2011).
35. T. Kim, H. Kang, S. Jeong, D. J. Kang, C. Lee, C. H. Lee, M. K. Seo, J. Y. Lee and B. J. Kim, ACS Appl. Mater. Interfaces, **6**, 16956 (2014).
36. R. Mueller, H. K. Kammler, S. E. Pratsinis, A. Vital, G. Beaucage and P. Burtscher, Powder Technol., **140**, 40 (2004).
37. H. K. Kammler, L. Mädler and S. E. Pratsinis, Chem. Eng. Technol., **24**, 583 (2001).
38. X. Guo, A. Gutsche, M. Wagner, M. Seipenbusch and H. Nirschl, J. Nanopart. Res., **15**, 1559 (2013).
39. S. Bau, O. Witschger, F. Gensdarmes and D. Thomas, J. Nanopart. Res., **14**, 1217 (2012).
40. H. M. Ryan, High Voltage Engineering and Testing, 2nd ed., The Institution of Electrical Engineers, London, England (2001).
41. ISO 14887:2000 (E). Sample Preparation - Dispersing Procedures for Powders in Liquids.
42. W. C. Hinds, Aerosol Technology: Properties, Behavior, and Measurement of Airborne Particles, 2nd ed., Wiley-Interscience, New York, USA (1999).
43. D. R. Lide, CRC handbook of chemistry and physics : a ready reference book of chemical and physical data, 86th ed., CRC Press, Boca Raton, USA (2005).
44. M. Ullmann, S. K. Friedlander and A. Schmidt-Ott, J. Nanopart. Res., **4**, 499 (2002).
45. S. K. Friedlander, Smoke, Dust, and Haze: Fundamentals of Aerosol Dynamics, 2nd ed., Oxford University Press, New York, USA (2000).
46. K. E. J. Lehtinen and M. R. Zachariah, J. Aerosol Sci., **33**, 357 (2002).
47. T. E. Itina and A. Voloshko, Appl. Phys. B, **113**, 473 (2013).
48. F. L. Jones, J. Appl. Phys., **1**, 60 (1950).
49. R. N. Szente, R. J. Munz and M. G. Drouet, J. Phys. D: Appl. hys., **27**, 1443 (1994).
50. M. S. Naidu and V. Kamaraju, High Voltage Engineering, 3rd ed., Tata McGraw-Hill Education, New Delhi, India (2004).
51. F. Llewellyn-Jones, M. A., D.Phil., D. Sc. and F. Inst. P., Platinum Metals Rev., **7**, 58 (1963).
52. W. Zhu and S. E. Pratsinis, ACS Symp. Ser., **662**, 64 (2009).
53. H. C. Oh, J. H. Ji, J. H. Jung and S. S. Kim, Mater. Sci. Forum, **544-545**, 143 (2007).
54. J. H. Byeon and Y. W. Kim, ACS Appl. Mater. Interfaces, **6**, 763 (2014).
55. X. Jing, J. H. Park, T. M. Peters and P. S. Thorne, Toxicol. In Vitro, **29**, 502 (2015).
56. S. Ghaemi, A. Schmidt-Ott and F. Scarano, Meas. Sci. Technol., **21**, 105403 (2010).